Received: 11 March 2021 | Revised: 25 June 2021 | Accepted: 19 July 2021

DOI: 10.1002/mgg3.1775

Molecular Genetics & Genomic Medicine Open Access WILEY

ORIGINAL ARTICLE

CRISPR/Cas9 in zebrafish: An attractive model for FBN1 genetic defects in humans

Xiaoyun Yin[1] | **Jianxiu Hao**[2] | **Yuanqing Yao**[1]

[1]Medical School of Chinese PLA, Beijing, China

[2]Clinical Biobank Center, the Medical Innovation Research Division, Chinese PLA General Hospital, Beijing, China

Correspondence
Yuanqing Yao, Medical School of Chinese PLA, No. 28, Fuxing Road, Haidian District, Beijing 100853, China.
Email: yaoyq@126.com (Y. Y.)

Funding Information
This work was supported by the Development and Standardization Research of Preimplantation Genetic Diagnosis (PGD) Technology (grant number 2018YFC1003100).

Abstract

Background: Mutations in the fibrillin-1 gene (*FBN1*) are associated with various heritable connective tissue disorders (HCTD). The most studied HCTD is Marfan syndrome. Ninety percent of Marfan syndrome is caused by mutations in the *FBN1* gene. The zebrafish share high genetic similarity to humans, representing an ideal model for genetic research of human diseases. This study aimed to generate and characterize *fbn1*$^{+/-}$ mutant zebrafish using the CRISPR/Cas9 gene-editing technology.

Methods: CRISPR/Cas9 was applied to generate an *fbn1* frameshift mutation (*fbn1*$^{+/-}$) in zebrafish. F1 *fbn1*$^{+/-}$ heterozygotes were crossed with transgenic fluorescent zebrafish to obtain F2 *fbn1*$^{+/-}$ zebrafish. Morphological abnormalities were assessed in F2 *fbn1*$^{+/-}$ zebrafish by comparing with the Tuebingen (TU) wild-type controls at different development stages.

Results: We successfully generated a transgenic line of *fbn1*$^{+/-}$ zebrafish. Compared with TU wild-type zebrafish, F2 *fbn1*$^{+/-}$ zebrafish exhibited noticeably decreased pigmentation, increased lengths, slender body shape, and abnormal cardiac blood flow from atrium to ventricle.

Conclusion: We generated the first *fbn1*$^{+/-}$ zebrafish model using CRISPR/Cas9 gene-editing approach to mimic *FBN1* genetic defects in humans, providing an attractive model of Marfan syndrome and a method to determine the pathogenicity of gene mutation sites.

KEYWORDS
animal model, CRISPR/Cas9, fibrillin-1, Marfan syndrome, zebrafish

1 | INTRODUCTION

Human *FBN1* (https://www.ncbi.nlm.nih.gov/gene/2200, updated on June 11, 2021) encodes a ~320 kDa extracellular matrix (ECM) protein fibrillin-1 that is widely expressed throughout the body and constitutes the backbone of microfibrils in the ECM (Jensen & Handford, 2016; Schrenk et al., 2018; Zigrino & Sengle, 2019). It contains three cysteine-rich repeating motifs (Jensen & Handford, 2016; Schrenk et al., 2018), which are epidermal growth factor (EGF) motifs and latent transformation growth factor-β1 binding protein (LTBP or TB) motifs and Fib motifs. The Fib motif is a unique hybrid motif of *FBN1*, which is formed by the fusion of EGF and LTBP

motifs. Among them, there are a total of 47 EGF motifs, of which 43 are calcium-binding epidermal growth factor (cbEGF) motifs that can bind to calcium ions. The *FBN1* protein contains 7 LTBP motifs. The above three motifs play an important role in maintaining the structure and protein function of *FBN1* (Jondeau et al., 2011; Jones & Ikonomidis, 2010; Ramirez & Pereira, 1999; Rantamäki et al., 1997; Robinson et al., 2006). Mutations in *FBN1* are associated with various heritable connective tissue disorders (HCTD), such as Marfan syndrome (MFS; Gong et al., 2019; Jondeau et al., 2017), Weill-Marchesani syndrome (WMS; Karoulias et al., 2020; Newell et al., 2017), Shprintzen-Goldberg syndrome (SGS; Bari et al., 2019), MASS phenotype (mitral valve prolapse, non-progressive aortic enlargement, skin changes and scoliosis, thoracic deformities and joint hyperactivity; Piqueras-Flores et al., 2019), and Neonatal Progeroid syndrome (Muthu & Reinhardt, 2020), accounting for ~90% of MFS cases. Mutations in the *FBN1* gene can also be found in other fibrillinopathy that does not meet the diagnostic criteria of MFS (non-syndrome), such as isolated ectopia lentis or congenital ectopia lentis (Cao et al., 2019; Yang et al., 2020; Zhang et al., 2018), familial thoracic aortic aneurysm and dissection (Arnaud et al., 2019; Takeda & Komuro, 2019), isolated skeletal features (Lin, Zhao, et al., 2020; Smaldone & Ramirez, 2016; Vasques et al., 2019), and so on. To date, more than 3000 mutations have been identified in *FBN1* and are generally classified into missense mutations, frameshift mutations, nonsense mutations, splicing mutations, and inframe deletions or insertions (Arnaud et al., 2017; Gong et al., 2019; Lin, Liu, et al., 2020; Xu et al., 2020). Most of the mutations lead to a wide range of clinical manifestations involving the integumentary, skeletal, ocular, central nervous, and cardiovascular systems, from hypopigmented or hyperpigmented scars, tall stature resulting from the overgrowth of the long bones in the limbs, to life-threatening cardiovascular abnormalities, suggesting complicate genotype-phenotype correlations in connective tissue disorders resulting from *fbn1* mutation (Sakai et al., 2016). MFS is a euchromatic dominant genetic disease with incomplete penetrance. The clinical phenotype is complex and the variability is large. There are large phenotypic differences between different families and even different patients of the same family. At present, more than 1,700 *FBN1* gene mutations (Bitterman & Sponseller, 2017; Groth et al., 2017; Li et al., 2017) have been discovered that can lead to MFS. Exons can also be lost during the splicing process of transcription products. The mutation sites are randomly distributed in each exon of the entire *FBN1* gene, and there are no obvious mutation hotspots; 20%–35% are scattered cases caused by new mutations. Most studies (Mastromoro et al., 2021; Tognato et al., 2019) have shown that exons 24–32 of the *FBN-1* gene encode the 11th–18th cbEGF and the third LTBP domain and its mutations are often associated with neonatal Marfan syndrome (nMFS). nMFS is the most serious type of MFS. Patients suffer from mitral valve or tricuspid valve insufficiency at birth or shortly after birth, and usually die within one year after birth. Severe congestive heart failure is the main cause of death. In addition, some severe phenotypes of classic MFS and non-classical MFS (Damrauer et al., 2019; Milleron et al., 2020) are also associated with mutations in this region, suggesting complicate genotype-phenotype correlations in MFS.

According to NCBI database, 310 organisms have orthologs with human *FBN1*, such as mouse, rat, pig, and zebrafish (https://www.ncbi.nlm.nih.gov/gene/?term=ortholog_gene_2200 [group]. Accessed 14 February 2021). Numerous studies have used mouse models to investigate *FBN1* mutation in MFS (Hibender et al., 2019; Park et al., 2019; Sato et al., 2018; Tran et al., 2019). A study has reported a heterozygous *fbn1* mutant pig model that exhibits phenotypes resembling the symptoms of human MFS (Umeyama et al., 2016). However, considering the small number of offspring and relatively high cost, the application of mouse or pig model in the high-throughput genetic analysis is challenging. Recently, zebrafish has emerged as a popular vertebrate model for genetic research (Busse et al., 2020; Torraca & Mostowy, 2018). The advantages of zebrafish in human disease modeling include optical transparent embryos, high fecundity, low-cost husbandry, short life cycle, ease of experimental manipulations, as well as a high degree of homology with human genes (Fontana et al., 2018). Sequencing of zebrafish has revealed that ~70% of human genes have functional homologs in zebrafish (Howe et al., 2013), suggesting that zebrafish is an attractive model for most human genetic diseases. However, no reports are available regarding the generation of *fbn1* (https://www.ncbi.nlm.nih.gov/gene/100330961, updated on June 13, 2020) mutation models in zebrafish.

Recently, the clustered regularly interspaced short palindromic repeat (CRISPR)/CRISPR-associated protein 9 (Cas9) technology has achieved tremendous progress in genome editing and has been applied in zebrafish to alter gene transcription and function (Barman et al., 2020; Cornet et al., 2018; Gupta et al., 2019). A typical CRISPR/Cas9-mediated mutagenesis pipeline in zebrafish includes small guide RNA (sgRNA) design and generation, microinjection of a preassembled sgRNA/Cas9 complex in one-cell stage embryos (F0), and generation of F1 heterozygous carriers and F2 homozygous mutant larvae (Albadri et al., 2017; Hoshijima et al., 2019). Scientists have successfully applied this pipeline in generating mutant zebrafish models for various human diseases, such as autism spectrum disorder (Liu et al., 2018), genetic cardiovascular disorders (Tessadori et al., 2018), and liver diseases (Kim et al., 2019).

However, the application of CRISPR/Cas9 technology in generating *fbn1* mutant zebrafish has not been reported yet.

Based on the standards and guidelines for the interpretation of sequence variants of the College of Medical Genetics and Genomics and the Association for Molecular Pathology (2015; Richards et al., 2015), the evidence levels of mutation site analysis were as follows: PVS: very strong pathogenicity; PS: strong pathogenicity; PM: moderate pathogenicity; PP: supporting pathogenicity. The *FBN1* mutation has evidence of PS2+PM2+PP1+PP3+PP4. PS2 refers to a new mutation, detected by the proband, but not detected by the parents; PM2: in the ESP database, the Thousand People database, and the EAC database. The allele frequency is 0; PP1: mutations and diseases are co-segregated in the family; PP3: multiple computer simulation calculations predict harmful; and PP4: mutation-related diseases are highly consistent with clinical phenotypes. Therefore, we conclude from the evidence supporting *FBN1* mutation that its classification belongs to likely pathogenic, which can be used for prenatal diagnosis. The purpose of this study is to construct a zebrafish model with *fbn1* gene knockout by CRISPR/cas9 technology, so as to confirm whether the model exhibits phenotypes resembling the symptoms of human MFS. The significance of establishing such an *fbn1* gene knockout zebrafish model is to provide a model and method to determine the pathogenicity of *FBN1* gene mutation sites in clinic, which is used to be the evidence supporting *FBN1* mutation classification. With advantages of large number of offspring and relatively low cost, it also provides a model to investigate *FBN1* mutation in MFS.

In this study, we generated and characterized the first CRISPR/Cas9-mediated loss-of-functional *fbn1* mutation ($fbn1^{+/-}$) model in zebrafish.

2 | MATERIALS AND METHODS

2.1 | Zebrafish care and husbandry

TU wild-type zebrafish and transgenic *Tg (cmlc2:eGFP)* zebrafish possessing a green fluorescent heart (Siegert et al., 2018) were obtained from Model Animal Research Center of Nanjing University (Nanjing Jiangsu, China). Embryos were treated with 0.003% tyrosine inhibitor 1-phenyl-2-thio-urea (cat# P7629-10G, Sigma-Aldrich) to inhibit pigment formation. The fish were maintained at 26 ± 2°C under a 14 hr light: 10 hr dark cycle in a zebrafish circulation breeding system (ESON; Beijing Aisheng Technology Development Co., Ltd.). To generate offspring, mating was carried out at a ratio of 1:1, followed by natural spawning.

2.2 | Generation of Cas9 transgenic zebrafish

fbn1 gene has not been sequenced in many databases, this design is based on NCBI database (https://www.ncbi.nlm.nih.gov/gene/XM_017351990.2). *fbn1* sgRNAs (CRISPR1: TGCGGAAGAGCTTGTGCTACAGG; CRISPR2: TCCGACAACGCCACATGTGACGG; CRISPR3: CCAGGCGCGGCCGATGTTGTAGG; CRISPR4: GGGAACGGGACACTTCTCGCAGG) were designed and synthesized by Nanjing YSY Biotech Company. The target sequences are in exon 16, near to the 1731st amino acid. A mixture (1 nl) of each sgRNA (80–100 ng/μl) and Cas9 protein (200 ng/μl; cat# P-020, Nanjing YSY Biotech) was injected into embryos (F0). The F0 embryos injected with Cas9/sgRNA were raised to sexual maturity, and four pairs of female and male zebrafish were mated to obtain F1 embryos.

2.3 | Genotyping of transgenic zebrafish

Genomic DNA was obtained from F1 embryos at 24 hr post-fertilization (hpf) for genotyping using the forward (5′-GAATCCTGGCATCTGTGGTC-3′) and reverse (5′-TTGCGCAAATCTTCTACTCAAA-3′) primers. The PCR protocol was 95°C for 3 min, 30 cycles of 95°C for 30 s, 62°C for 30 s and 72°C for 1 min, and 72°C for 10 min. PCR products were sequenced to identify the mutation. F0 with heritable mutations were selected to mate to generate F1 offspring, followed by genomic DNA collection at 2 months post-fertilization for genotyping. PCR reaction was performed using the primers and PCR protocol mentioned above, followed by sequencing. To confirm the genotype carried by the mutants, the PCR products of mutant 1 and mutant 2 carrying the *fbn1* frameshift mutation were recombined into the pGEM-T Easy vector. After transformation, a single colony was selected for PCR identification. The confirmed F1 $fbn1^{+/-}$ heterozygotes were used in the following investigation.

2.4 | Morphology assessment

The F1 adult $fbn1^{+/-}$ zebrafish were mated with *Tg(cmlc2:eGFP)* fish to generate F2 transgenics. The morphology of F2 embryos/larvae and TU control group were examined at 72 hpf, 120 hpf, 12 dpf, 19 dpf, 26 dpf, 33 dpf, and 40 dpf using a stereomicroscope (MC50-S; Mingmei). Images were acquired using an SZX7 camera (Olympus). The initial sample size was 310 in F2 $fbn1^{+/-}$ zebrafish experimental group and TU control group, respectively. The death rate was about 3%. The abnormal phenotypes of the F2 and TU groups were analyzed statistically. The experiment was repeated three times.

2.5 | All reagents used in the experiment include the following

YSY buffer (cat# R-001, Nanjing YSY Biotech), Zebrafish genotyping kit (cat# K-101, Nanjing YSY Biotech), 2-Mastermix (cat# P111-01, Vazyme Biotech Co., Ltd), Ultrapure water without ribozyme pollution (cat# R-002, Nanjing YSY Biotech), 1-phenyl-2-thiourea (cat# P7629-10G, Sigma-Aldrich), T7 in vitro Transcription Kit (cat# P7629-10G, TaKaRa), MAXIscript SP6/T7 (cat# AM1314, Ambion), PCR clean up Kit (cat# AP-MN-P-250, Axygen), DL5000 marker (cat#3428A, TaKaRa), Ampicillin (cat# A610028, Sangon Biotech Co., Ltd), DNase I (cat# 2238G2, Ambion), PCR-related reagent T4 ligase (cat# M0202L, New England Biolabs), PGEM-Teasy Vector (cat# A1360, Nanjing YSY Biotech), Cas9 protein (cat# P-020, Nanjing YSY Biotech), Conventional chemical reagent (cat# 10010360, cat# 30148126, cat# 71001453, Shanghai Chemical Reagent, Co., Ltd; cat#34943-6X1L, cat#296821-1L, cat# 284505-2L, Sigma Aldrich).

2.6 | Ethical Compliance and Ethical Considerations

The animal protocol was approved by an ethics committee of the Institutional Animal Care and Use Committee of The 1st Medical Center of Chinese PLA General Hospital (Beijing, China). All animal experiments were performed following the guidelines for animal welfare in Laboratory of Translational Medicine of The 1st Medical Center of Chinese PLA General Hospital.

3 | RESULTS

3.1 | Generation of *fbn1*$^{+/-}$ zebrafish

By comparative analyses using NCBI and Ensembl resources, we found that *fbn1* is orthologous between humans and zebrafish (Figure S1), suggesting that zebrafish is an ideal model for genetic research on *fbn1* mutation. To establish an *fbn1* mutant zebrafish

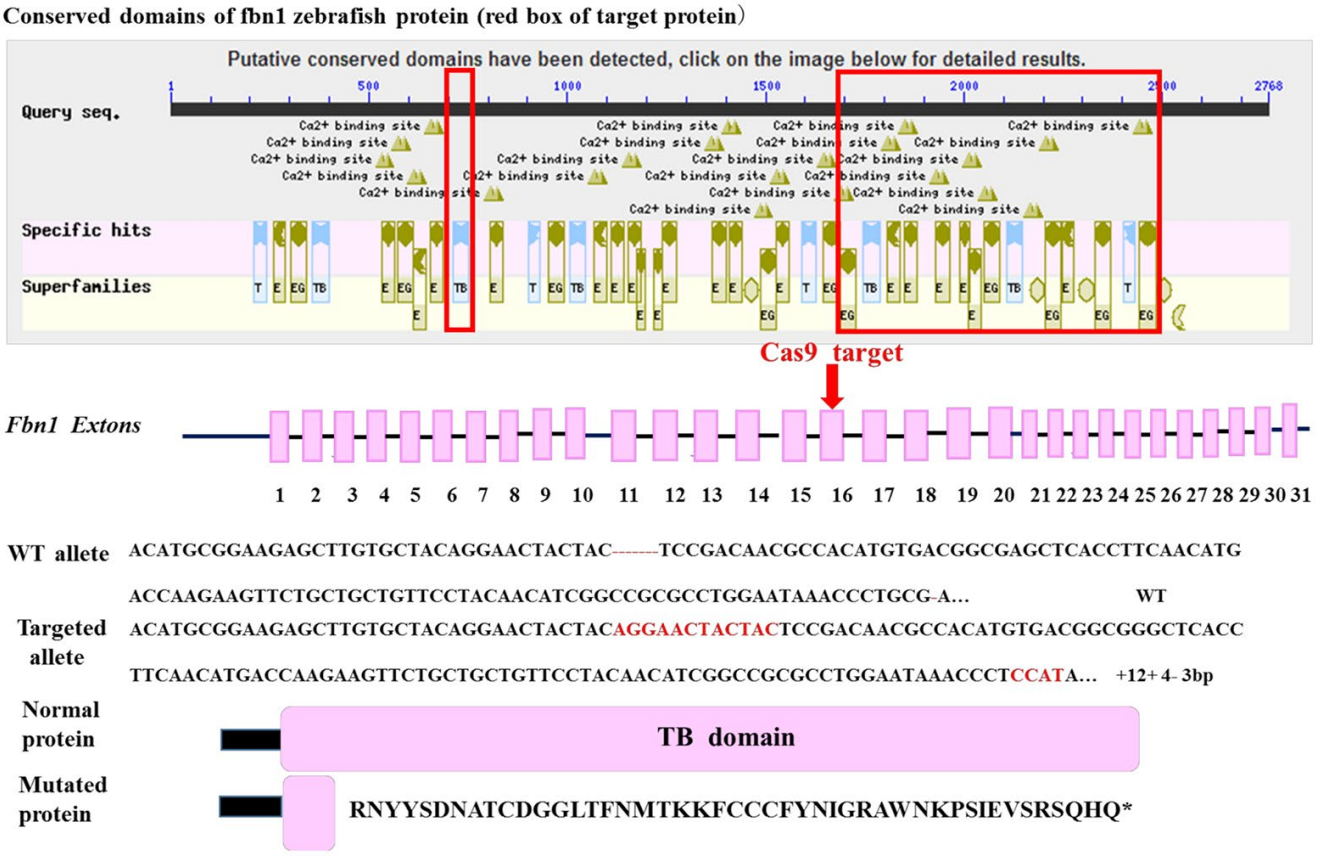

FIGURE 1 FIGURE Generation of *fbn1*$^{+/-}$ zebrafish. The conserved domains of *FBN1* protein in zebrafish are shown. The red box and the red arrow indicate the target of CRISPR/Cas9 gene editing. The CRISPR/Cas9 induced a frameshift mutation containing 3-base deletion and 16-base insertion in *fbn1*. The inserted nucleotides are marked in red. The red dashed line indicates the 3-base deletion. WT: wildtype; TB: transforming growth factor-beta-binding protein-like

model, we designed 4 sgRNAs in exon 16 of *fbn1* and tested their efficiency by co-injecting with Cas9 protein into one-cell stage zebra embryos (Figure S2). DNA sequencing of target-specific PCR products confirmed that the *fbn1* targeted allele carried a deletion of 3 bases and an insertion of 16 bases, resulting in a frameshift mutation and truncated *FBN1* protein after the mutation (Figure 1). PCR analysis showed that the wildtype allele generated a band of 338 bp, whereas the mutant allele generated two bands of 351 bp and 338 bp (Figure 2a). Then, we generated F2 transgenics fish by mating adult F1 *fbn1*$^{+/-}$ fish with *Tg(cmlc2:eGFP)* fish. PCR analysis and sequencing confirmed that the randomly selected F2 *fbn1*$^{+/-}$ heterozygous mutants carried the mutations (Figure 2b–e). These results suggest that we successfully generated a transgenic line of *fbn1*$^{+/-}$ zebrafish.

3.2 | F2 *fbn1*$^{+/-}$ zebrafish exhibits morphological and cardiac defects

Then, we examined whether our transgenic zebrafish exhibit abnormal phenotypes of connective tissue genetic diseases. Figure 3 shows the morphology of F2 *fbn1*$^{+/-}$ zebrafish in the early stage of development (72 and 120 hpf). Figure 4 shows that compared with TU wildtype zebrafish, F2 *fbn1*$^{+/-}$ zebrafish exhibited noticeably decreased pigmentation, increased body lengths, cardiac defects (abnormal cardiac blood flow from atrium to ventricle) and slender body shape. Some F2 *fbn1*$^{+/-}$ zebrafish appeared more transparent and slender at 40 dpf than those at earlier developmental stages.

The dynamic video demonstrated abnormal cardiac blood flow from atrium to ventricle in F2 *fbn1*$^{+/-}$ zebrafish throughout the developmental stages. In addition, F2 *fbn1*$^{+/-}$ zebrafish at 33 and 40 dpf showed less and slower

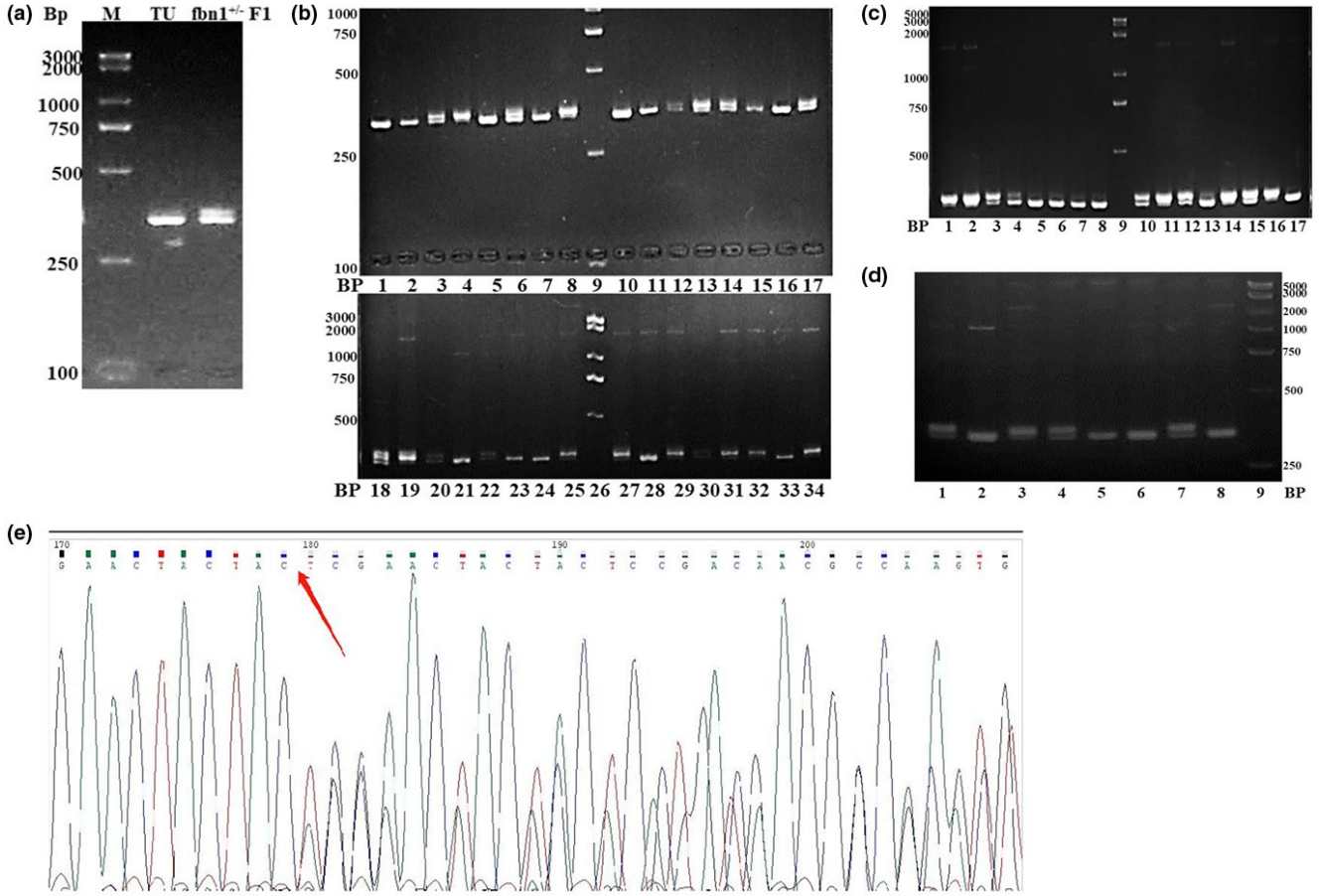

FIGURE 2 FIGURE Identification of F2 *fbn1*$^{+/-}$ zebrafish. (a) PCR amplification of the genomic DNA from TU wild-type and F1 *fbn1*$^{+/-}$ zebrafish. M, DNA marker. (b–d) PCR amplification of the genomic DNA of F2 *fbn1*$^{+/-}$ adults. Lanes 9 and 26, DNA Marker; lanes 3, 4, 6, 8, 12–14, 17, 18–20, 22, 25, 27, 29–32, and 34 in (b), heterozygous for alleles A and B mutants; lanes 1, 2, 5, 7, 9–11, 15, 16, 21, 23, 24, 26, 28, and 33 in (b), wild-type; lanes 1–3, 10–12, 14–16 in (c), heterozygous mutants of alleles A and B; lanes 4–9, 13, and 17 in (c), wild-type; lanes 1, 3, 4, and 7 in (D), heterozygous mutants of alleles A and B; lanes 2, 5, 6, 8, and 9 in (d), wild-type. (e) DNA sequencing results of F2 fbn1$^{+/-}$ fish. Red arrow indicates the position of the mutation

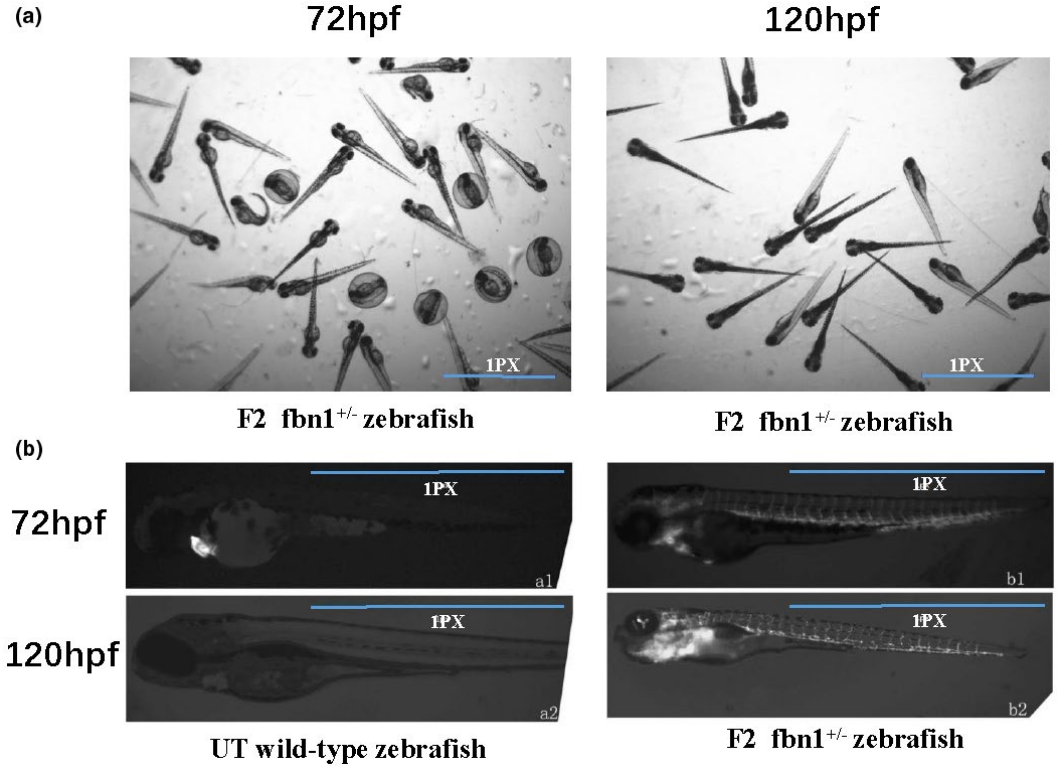

FIGURE 3 (a) Represents the "family portrait" of the F2 *fbn1*$^{+/-}$ zebrafish (experimental group) generated by the hybridization of F1 *fbn1*$^{+/-}$ heterozygous mutants and Tg(cmlc2:eGFP) transgenic fluorescent zebrafish. The picture on the left is the morphology of F2 *fbn1*$^{+/-}$ zebrafish at 72 hr post-fertilization, and the picture on the right is a 120-hr "family portrait" of F2 *fbn1*$^{+/-}$ zebrafish. In (b) group a is the fluorescence micrograph of TU wild-type embryos, and group b is the fluorescence micrograph of F2 embryos (experimental group), where a1 and b1 are 72 hr fluorescence images, a2 and b2 are 120 hr fluorescence images. The results showed that no significant difference was found in the early developmental observation between the TU wild-type and F2 generation experimental groups. The legend has been marked with the meaning of "a1, a2, b1, b2." Scale bars have been marked in Figure 3. Magnification eyepiece ×0.6 (A) and eyepiece ×2.0 (B). hpf: hours post-fertilization

cardiac blood flow compared with the wild-type zebrafish. Taken together, these findings suggest that *fbn1*$^{+/-}$ zebrafish exhibit typical features for connective tissue genetic diseases due to *FBN1* mutations.

3.3 | Statistical results of abnormal phenotypes in F2 and TU groups:

The initial sample size was 310 in F2 fbn1$^{+/-}$ zebrafish experimental group and TU control group, respectively. The death rate was about 3%. The experiment was repeated three times. The abnormal phenotypes of F2 and TU groups were analyzed statistically. The body length (unit: mm), melanin reduction, and cardiac defects were observed in TU (control group) and F2 (experimental group) at 12 dpf/19 dpf/26 dpf/33 dpf/40 dpf. The two abnormal phenotypes of melanin reduction and cardiac defect were observed in three visual fields, each with about 100 samples. The statistical software was SPSS 22.0. There was statistical significance when $p < .05$.

T-test was used to analyze the body length data of F2 and TU control groups. The results of three experiments showed that the body length of F2 group was significantly longer than that of TU group at 12 dpf, 19 dpf, and 26 dpf ($p < .05$); In the second experiment, F2 group compared with TU control group at 40 dpf, $p = .952$, without statistical significance; In the third experiment, F2 group compared with TU group at 33 dpf, $p = .164$, without statistical significance. In short, the body length of F2 *fbn1*$^{+/-}$ zebrafish increased significantly throughout the developmental stages, especially at the early stage (Table 1).

Chi-square test was used to analyze the data of hypopigmentation and cardiac defects in F2 and TU control groups at 12 dpf/19 dpf/26 dpf/33 dpf/40 dpf. The results of three experiments showed that the pigmentation of F2 group was significantly lower than that of TU group at 12 dpf, 19 dpf, and 26 dpf ($p < .05$) and there was no significant difference between F2 and TU groups at 40 dpf ($p > .05$). According to the results of the first and second experiments, there was no significant difference at 33 dpf ($p > .05$). The above results showed that the level of

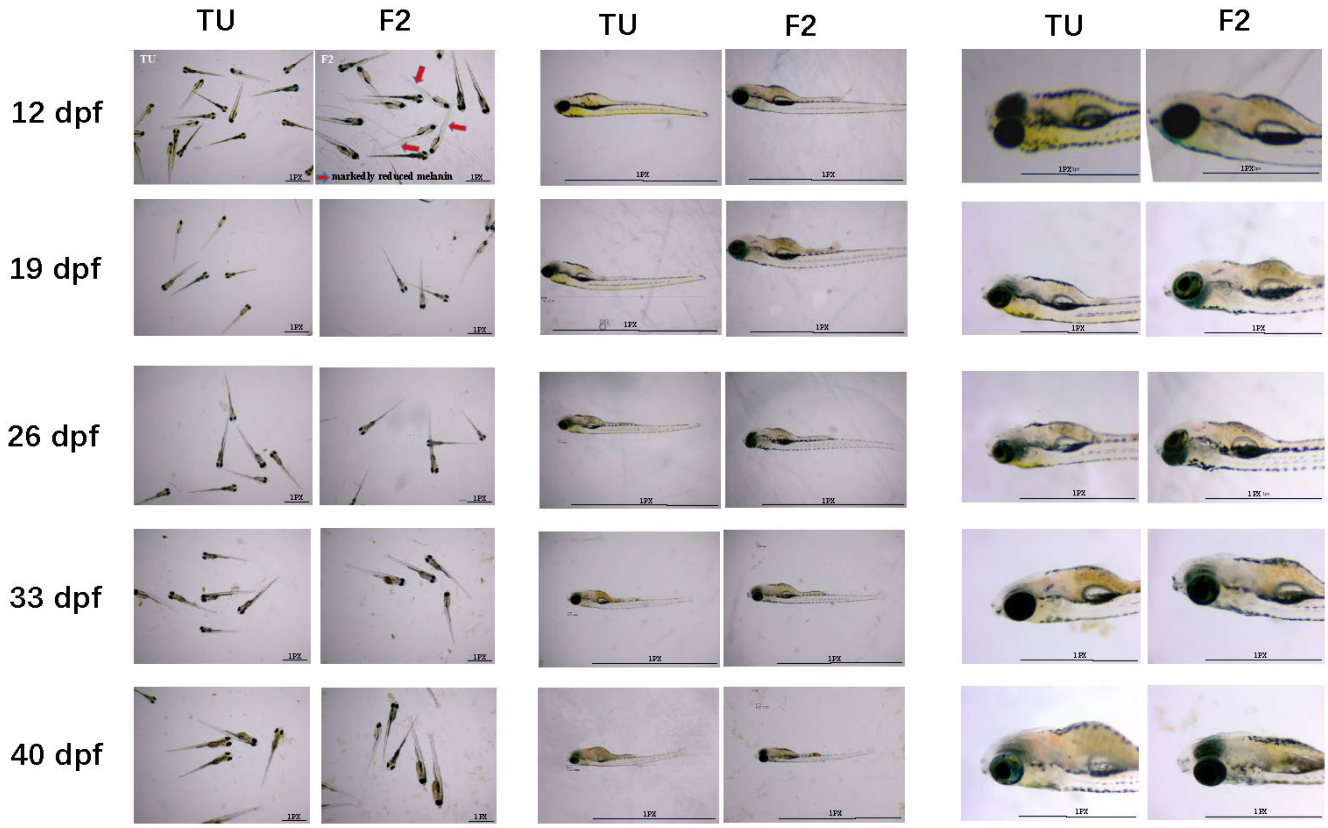

FIGURE 4 Comparison of the morphology, head, and heart between F2 *fbn1*$^{+/-}$ and TU wild-type zebrafish larvae. Representative images of the morphology of F1 and F2 *fbn1*$^{+/-}$ zebrafish at 12, 19, 26, 33, and 40 days post-fertilization are shown. F2 *fbn1*$^{+/-}$zebrafish exhibited more noticeably decreased melanin, the red arrow in the figure refers to the typical representatives of F2 embryos showing the characteristics of markedly reduced melanin at the 12 days post-fertilization. Scale bars have been marked in Figure 4. Magnification eyepiece ×0.6 (left), ×1.0–2.0 (middle), and ×3.5 (right). dpf: days post-fertilization

pigmentation of F2 group decreased significantly at the early stage (12 dpf/19 dpf/26 dpf), but there was no significant difference between the two groups at the later stage (Table 2). The statistical results of the three experiments showed that F2 had significant heart defects compared with TU control group at 12 dpf/19 dpf/26 dpf/33 dpf/40 dpf ($p < .05$; Table 3).

4 | DISCUSSION

MFS is characterized by pleiotropic manifestations at least partially due to the great number of mutations identified in *FBN1* (Gong et al., 2019; Jondeau et al., 2017). The pathogenesis of MFS was secondary to the mutation of *FBN1* gene, which resulted in the dysfunction of the structure and function of the extracellular matrix, and then the loss of connective tissue integrity (Gong et al., 2019; Jondeau et al., 2017). Many studies (De Cario et al., 2018; Siegert et al., 2018; Takeda et al., 2018) have shown that *FBN1 protein* is related to transforming growth factor-β (TGF-β) signal transduction function in the extracellular matrix. Mutations in the *FBN1* gene can make TGF-β signal transduction dysregulated, and the pathogenesis of MFS may be related to abnormal TGF-β signaling. A large-scale genotype–phenotype mapping is required for a better understanding of the contributions of *FBN1* mutations in MFS. Compared with the most popular model organism mouse that has a relatively small number of offspring and expensive husbandry, the zebrafish has become a better model organism for large-scale genetics projects (Busse et al., 2020; Torraca & Mostowy, 2018; Varshney et al., 2015). In this study, we generated the first *fbn1*$^{+/-}$ zebrafish model using the CRISPR/Cas9 gene-editing tool and characterized the morphological and cardiovascular abnormalities of *fbn1*$^{+/-}$ zebrafish at the larval stage. The TB domain truncation resulting from *fbn1*$^{+/-}$ mutation caused noticeable hypopigmentation, increased length, slender body shape, and cardiovascular defects in zebrafish larvae, reminiscent of human MFS.

By comparing FBN1 protein sequences between human and zebrafish, we found that human FBN1 protein is highly conserved in zebrafish, consistent with previous reports (Cetinkaya et al., 2018; Gao et al., 2019). *FBN1* performs

similar functions among different species. As the major component of microfibrils that regulate elastic fiber formation, *FBN1* provides the scaffold for elastin deposition to maintain the structural integrity of the vessel wall during embryonic development and early postnatal life. The neonatal demise of *fbn1*$^{-/-}$mice due to ruptured aortic aneurysm suggests that *fbn1* is required for the blood vessel structure and function during neonatal life (Cook et al., 2012). Chen et al. have demonstrated that injection with morpholino antisense oligomers against *fbn1* into zebrafish embryos leads to dilated vessels around the eyes and in the head, suggesting that *fbn1* is essential for vascular development and function in zebrafish (E. Chen et al., 2006). Thus, it is reasonable to generate a zebrafish model to mimic *FBN1* genetic defects in humans.

Although zebrafish and humans share abouchomology, there are still big differences. So far, the most studied genotype–phenotype correlation is the 11–18 common sequence of cbEGF encoded by exon 24–32 and the third LTBP sequence of human *FBN1* gene related to nMFS, which is the most serious form of MFS. The original intention of this study is to use CRISPR/Cas9 technology to target the cbEGF sequence and the third LTBP sequence of zebrafish *fbn1* gene to simulate the zebrafish model of nMFS. However, we found that there are three cbEGF domains in zebrafish *fbn1* protein during CRISPR design, which are significantly different from the cbEGF domain of human *FBN1* protein. Moreover, the third LTBP domain of zebrafish *fbn1* protein is ahead. Therefore, we plan to knockout the third LTBP domain in *fbn1* protein, but because the blast of NCBI cannot give the genome sequence near the third LTBP domain (RID: 4yevbx78014), we change to knock out the cbEGF domain in *fbn1* protein. However, due to our previous knockout design in cbEGF domain of *fbn1* protein, we could not obtain sgRNA that could effectively guide Cas9 to cleave *fbn1*, so we abandoned the idea of zebrafish model simulating nMFS and replaced the design site. According to the results of NCBI blast alignment, zebrafish *fbn1* gene began to have genomic support in 1362aa. Considering that there are many repeats in the intron of the gene, in order to achieve gene knock out and avoid gene compensation, we designed the target sequence (CRISPR) of *fbn1* gene to be targeted near 1731aa (after the potential start codon). By causing frameshift mutation, we can achieve the goal of targeted knockout of *fbn1* gene.

In our study, the *fbn1* targeted allele carried a frameshift mutation containing a 3-base deletion and a 16-base insertion, resulting in a truncated *FBN1* with a loss of a TB domain after the mutation. This frameshift mutation might affect *FBN1* function by disrupting the protein structure or the binding of calcium with the cbEGF domain. It has been reported that of all the identified

TABLE 1 The statistical results of body length data of F2 and TU groups

	The first experiment			The second experiment			The third experiment		
Body length	**TU**	**F2**	***p***	**TU**	**F2**	***p***	**TU**	**F2**	***p***
12 dpf	310	310		310	310		310	310	
x ± s	4.50 ± 0.197	6.50 ± 0.235	<.001	4.81 ± 0.221	6.39 ± 0.246	<.001	4.60 ± 0.266	6.61 ± 0.265	<.001
19 dpf	308	306		306	306		307	308	
x ± s	8.50 ± 0.238	10.33 ± 0.204	<.001	8.70 ± 0.249	10.51 ± 0.254	<.001	8.55 ± 0.285	10.83 ± 0.396	<.001
26 dpf	305	304		303	304		305	305	
x ± s	13.67 ± 0.312	14.30 ± 0.428	<.001	13.69 ± 0.351	14.37 ± 0.456	<.001	13.84 ± 0.458	14.58 ± 0.479	<.001
33 dpf	303	302		301	302		303	302	
x ± s	19.01 ± 0.386	19.44 ± 0.448	<.001	19.50 ± 0.482	19.72 ± 0.526	<.001	20.16 ± 0.578	20.10 ± 0.474	.164
40 dpf	300	300		300	299		301	300	
x ± s	25.31 ± 0.530	25.57 ± 0.645	<.001	26.22 ± 0.570	26.22 ± 0.616	.952	27.12 ± 0.657	27.32 ± 0.766	.001

TABLE 2 The statistical results of decreased pigmentation of F2 and TU groups

Decreased pigmentation	The first experiment			The second experiment			The third experiment		
	TU	F2	*p*	TU	F2	*p*	TU	F2	*p*
12 dpf	310	310		310	310		310	310	
Percentage	34 (11.3%)	154 (49.7%)	<.001	31 (10.3%)	155 (50.6%)	<.001	34 (11.3%)	139 (44.8%)	<.001
19 dpf	308	306		306	306		307	308	
Percentage	30 (9.7%)	102 (33.3%)	<.001	34 (11.1%)	111 (36.3%)	<.001	32 (10.4%)	110 (35.7%)	<.001
26 dpf	305	304		303	304		305	305	
Percentage	26 (8.5%)	52 (17.1%)	.002	25 (8.3%)	60 (19.7%)	<.001	26 (8.5%)	57 (18.7%)	<.001
33 dpf	303	302		301	302		303	302	
Percentage	24 (7.9%)	38 (12.6%)	.059	23 (7.6%)	36 (11.9%)	.077	22 (7.3%)	45 (14.9%)	.003
40 dpf	300	300		300	299		301	300	
Percentage	26 (8.7%)	31 (10.3%)	.486	23 (7.7%)	27 (9.0%)	.546	23 (7.6%)	26 (8.7%)	.646

TABLE 3 The statistical results of cardiac defects of F2 and TU groups

Cardiac defects	The first experiment			The second experiment			The third experiment		
	TU	F2	*p*	TU	F2	*p*	TU	F2	*p*
12 dpf	310	310		310	310		310	310	
Percentage	13 (4.2%)	266 (85.8%)	<.001	13 (4.2%)	265 (85.5%)	<.001	10 (3.2%)	280 (90.3%)	<.001
19 dpf	308	306		306	306		307	308	
Percentage	10 (3.2%)	255 (83.3%)	<.001	11 (3.6%)	260 (85%)	<.001	6 (2.0%)	280 (90.9%)	<.001
26 dpf	305	304		303	304		305	305	
Percentage	8 (2.6%)	249 (81.9%)	<.001	8 (2.6%)	262 (86.2%)	<.001	8 (2.6%)	268 (87.9%)	<.001
33 dpf	303	302		301	302		303	302	
Percentage	8 (2.6%)	262 (86.8%)	<.001	9 (3.0%)	255 (84.4%)	<.001	8 (2.6%)	264 (87.4%)	<.001
40 dpf	300	300		300	299		301	300	
Percentage	5 (1.7%)	240 (80.0%)	<.001	5 (1.7%)	254 (84.9%)	<.001	4 (1.3%)	260 (86.7%)	<.001

FBN1 mutations, 38.6% lead to a truncated *FBN1* protein (Lin, Liu, et al., 2020). Studies have shown that truncating *FBN1* mutations is strongly associated with cardiovascular events in patients with MFS (M. Chen et al., 2018; Tan et al., 2017; Wang et al., 2016). Likewise, in our study, F2 *fbn1*$^{+/-}$ zebrafish larvae showed obviously abnormal phenotype of the heart. The dynamic video of the heart showed that the cardiac blood flow from atrium to ventricle in some F2 *fbn1*$^{+/-}$ zebrafish was different from that of the control group. The statistical results of the three experiments showed that F2 had significant heart defects compared with TU group at 12 dpf/19 dpf/26 dpf/33 dpf/40 dpf ($p < .05$; Table 3). In addition, F2 *fbn1*$^{+/-}$ zebrafish at 33 dpf and 40 dpf had less and slower cardiac blood flow compared with the control group. These results suggest that the *fbn1* mutation in our study affects cardiovascular development throughout the life span of the F2 *fbn1*$^{+/-}$ zebrafish and the abnormal cardiac phenotype gradually deteriorates with growth and development.

A study has reported that hypopigmented or hyperpigmented scars are present in 46% of patients with MFS versus 21% of control subjects (Ledoux et al., 2011). The abnormal pigmentation may be related to *SLC24A5*, which is 266 kb upstream of *FBN1* in the human genome and plays a key role in skin pigmentation in humans as well as in zebrafish (Lamason et al., 2005). Similar to that observed in humans, our results showed that F2 *fbn1*$^{+/-}$ zebrafish exhibited noticeably decreased pigmentation in the larval stage. Fibrillin scaffolds contribute to TGF-β/bone morphogenetic protein signaling during bone growth and metabolism. Despite the low abundance of fibrillins in skeletal tissues, mutations in *FBN1* or *FBN2* lead to skeletal abnormalities (Smaldone & Ramirez, 2016; Xu et al., 2019). As a result, tall, thin body habitus and long limbs are typical skeletal characteristics in patients with MFS (Sivasankari et al., 2017). To evaluate whether *fbn1* mutation in this study can mimic *FBN1* genetic defects in the human skeletal system, we measured the length of zebrafish and found that F2 *fbn1*$^{+/-}$ zebrafish exhibited

noticeably increased lengths and slender body shape compared with the wildtype counterparts. The statistical results of three experiments showed that the body length of F2 *fbn1*$^{+/-}$ zebrafish increased significantly throughout the developmental stages, especially at the early stage (Table 1). The statistical results showed that the level of pigmentation of F2 group decreased significantly at the early stage (12 dpf/19 dpf/26 dpf), but there was no significant difference between the two groups at the later stage (Table 2). Some F2 *fbn1*$^{+/-}$ zebrafish looked more transparent and more slender at 40 dpf. It is suggested that there is a certain phenotypic difference between the F2 generation and the two phenotypes of "increased body lengths and cardiac defects" are widespread, and the heart abnormality gradually deteriorates. The biggest difference between the zebrafish phenotype after *fbn1* gene knockout and human MFS patients is that there is no abnormality in the retina of F2 *fbn1*$^{+/-}$ zebrafish. Human MFS most often involves cardiovascular, skeletal, and ocular systems. The most common ocular manifestations of MFS are lens dislocation (mild eversion, accounting for about 60%), early and severe myopia, retinal detachment, early attack of cataract or glaucoma, corneal flattening, and iris hypoplasia also occur (Busse et al., 2020; Karoulias et al., 2020). The histological differences of the eyes, especially the retina between the experimental group and the control group need to be further studied. Unfortunately, due to the problem of experimental funding, no follow-up study has been carried out, which will be the focus of our next research. In short, these findings collectively suggest that our *fbn1*$^{+/-}$ zebrafish mutants could morphologically mimic the clinical features of MFS. Besides, similar to MFS, there is a certain phenotypic difference between the F2 *fbn1*$^{+/-}$ mutants and the abnormal cardiac phenotype gradually deteriorates with growth and development.

5 | CONCLUSIONS

In this study, using the CRISPR/Cas9 gene-editing tool, we successfully generated the first *fbn1*$^{+/-}$ zebrafish model that displays significant morphological and cardiovascular abnormalities reminiscent of MFS. Our findings may provide an efficient model for further study of the gene function of *FBN1* and a method to determine the pathogenicity of gene mutation sites.

CONFLICT OF INTEREST

The authors declare no conflict of interest.

AUTHOR CONTRIBUTIONS

Yuanqing Yao designed the study. Xiaoyun Yin performed the experiments, interpreted the data, and wrote the manuscript. Xiaoyun Yin and Jianxiu Hao carried out some of the experiments and participated in data analyses and interpretation, critically revised the manuscript. All authors read and approved the final manuscript.

ETHICAL APPROVAL

The animal protocol was approved by the Institutional Animal Care and Use Committee of The 1st Medical Center of Chinese PLA General Hospital (Beijing, China). All animal experiments were performed following the guidelines for animal welfare in Laboratory of Translational Medicine of The 1st Medical Center of Chinese PLA General Hospital.

DATA AVAILABILITY STATEMENT

The data underlying this article are available in the article and in its online supplementary material.

ORCID

Xiaoyun Yin https://orcid.org/0000-0002-8522-6361

REFERENCES

Albadri, S., Del Bene, F., & Revenu, C. (2017). Genome editing using CRISPR/Cas9-based knock-in approaches in zebrafish. *Methods*, *121–122*, 77–85. https://doi.org/10.1016/j.ymeth.2017.03.005

Arnaud, P., Hanna, N., Aubart, M., Leheup, B., Dupuis-Girod, S., Naudion, S., & Boileau, C. (2017). Homozygous and compound heterozygous mutations in the FBN1 gene: Unexpected findings in molecular diagnosis of Marfan syndrome. *Journal of Medical Genetics*, *54*(2), 100–103. https://doi.org/10.1136/jmedgenet-2016-103996

Arnaud, P., Hanna, N., Benarroch, L., Aubart, M., Bal, L., Bouvagnet, P., Busa, T., Dulac, Y., Dupuis-Girod, S., Edouard, T., Faivre, L., Gouya, L., Lacombe, D., Langeois, M., Leheup, B., Milleron, O., Naudion, S., Odent, S., Tchitchinadze, M., … Boileau, C. (2019). Genetic diversity and pathogenic variants as possible predictors of severity in a French sample of nonsyndromic heritable thoracic aortic aneurysms and dissections (nshTAAD). *Genetics in Medicine*, *21*(9), 2015–2024. https://doi.org/10.1038/s41436-019-0444-y

Bari, A., Sadaqat, N., Nawaz, N., & Bano, I. (2019). Shprintzen-goldberg syndrome: A rare disorder. *Journal of the College of Physicians and Surgeons Pakistan*, *29*(6), S41–S42. https://doi.org/10.29271/jcpsp.2019.06.S41

Barman, A., Deb, B., & Chakraborty, S. (2020). A glance at genome editing with CRISPR-Cas9 technology. *Current Genetics*, *66*(3), 447–462. https://doi.org/10.1007/s00294-019-01040-3

Bitterman, A. D., & Sponseller, P. D. (2017). Marfan syndrome: A clinical update. *Journal of American Academy of Orthopaedic Surgeons*, *25*(9), 603–609. https://doi.org/10.5435/jaaos-d-16-00143

Busse, B., Galloway, J. L., Gray, R. S., Harris, M. P., & Kwon, R. Y. (2020). Zebrafish: An emerging model for orthopedic research. *Journal of Orthopaedic Research*, *38*(5), 925–936. https://doi.org/10.1002/jor.24539

Cao, Q., Xiao, B., Jin, G., Lin, J., Wang, Y., Young, C., Lin, J., Zhou, Y., Zhang, B. O., Cao, M., Wu, K., & Zheng, D. (2019). Expression of transforming growth factor β and matrix metalloproteinases in the aqueous humor of patients with congenital ectopia lentis. *Molecular Medicine Reports*, *20*(1), 559–566. https://doi.org/10.3892/mmr.2019.10287

Cetinkaya, A., Karaman, A., Mutlu, M. B., & Yavuz, T. (2018). Novel FBN1 mutation in a family with inherited Marfan Syndrome: p.Cys2672Arg. *Congenital Anomalies (Kyoto)*, *58*(1), 41–43. https://doi.org/10.1111/cga.12220

Chen, E., Larson, J. D., & Ekker, S. C. (2006). Functional analysis of zebrafish microfibril-associated glycoprotein-1 (Magp1) in vivo reveals roles for microfibrils in vascular development and function. *Blood*, *107*(11), 4364–4374. https://doi.org/10.1182/blood-2005-02-0789

Chen, M., Yao, B., Yang, Q., Deng, J., Song, Y., Sui, T., Zhou, L., Yao, H., Xu, Y., Ouyang, H., Pang, D., Li, Z., & Lai, L. (2018). Truncated C-terminus of fibrillin-1 induces Marfanoid-progeroid-lipodystrophy (MPL) syndrome in rabbit. *Disease Models & Mechanisms*, *11*(4), dmm031542. https://doi.org/10.1242/dmm.031542

Cook, J. R., Smaldone, S., Cozzolino, C., del Solar, M., Lee-Arteaga, S., Nistala, H., & Ramirez, F. (2012). Generation of Fbn1 conditional null mice implicates the extracellular microfibrils in osteoprogenitor recruitment. *Genesis*, *50*(8), 635–641. https://doi.org/10.1002/dvg.22022

Cornet, C., Di Donato, V., & Terriente, J. (2018). Combining Zebrafish and CRISPR/Cas9: Toward a more efficient drug discovery pipeline. *Frontiers in Pharmacology*, *9*, 703. https://doi.org/10.3389/fphar.2018.00703

Damrauer, S. M., Hardie, K., Kember, R. L., Judy, R., Birtwell, D., Williams, H., & Pyeritz, R. E. (2019). FBN1 coding variants and nonsyndromic aortic disease. *Circulation Genomic and Precision Medicine*, *12*(6), e002454. https://doi.org/10.1161/circgen.119.002454

De Cario, R., Sticchi, E., Lucarini, L., Attanasio, M., Nistri, S., Marcucci, R., Pepe, G., & Giusti, B. (2018). Role of TGFBR1 and TGFBR2 genetic variants in Marfan syndrome. *Journal of Vascular Surgery*, *68*(1), 225–233.e225. https://doi.org/10.1016/j.jvs.2017.04.071

Fontana, B. D., Mezzomo, N. J., Kalueff, A. V., & Rosemberg, D. B. (2018). The developing utility of zebrafish models of neurological and neuropsychiatric disorders: A critical review. *Experimental Neurology*, *299*(Pt A), 157–171. https://doi.org/10.1016/j.expneurol.2017.10.004

Gao, L., Tian, T., Zhou, X., Fan, L., Wang, R., & Wu, H. (2019). Detection of ten novel FBN1 mutations in Chinese patients with typical or incomplete Marfan syndrome and an overview of the genotype-phenotype correlations. *International Journal of Cardiology*, *293*, 186–191. https://doi.org/10.1016/j.ijcard.2019.06.066

Gong, B., Yang, L., Wang, Q., Ye, Z., Guo, X., Yang, C., & Yang, Z. (2019). Mutation screening in the FBN1 gene responsible for Marfan syndrome and related disorder in Chinese families. *Molecular Genetics & Genomic Medicine*, *7*(4), e00594. https://doi.org/10.1002/mgg3.594

Groth, K. A., Von Kodolitsch, Y., Kutsche, K., Gaustadnes, M., Thorsen, K., Andersen, N. H., & Gravholt, C. H. (2017). Evaluating the quality of Marfan genotype-phenotype correlations in existing FBN1 databases. *Genetics in Medicine*, *19*(7), 772–777. https://doi.org/10.1038/gim.2016.181

Gupta, D., Bhattacharjee, O., Mandal, D., Sen, M. K., Dey, D., Dasgupta, A., Kazi, T. A., Gupta, R., Sinharoy, S., Acharya, K., Chattopadhyay, D., Ravichandiran, V., Roy, S., & Ghosh, D. (2019). CRISPR-Cas9 system: A new-fangled dawn in gene editing. *Life Sciences*, *232*, 116636. https://doi.org/10.1016/j.lfs.2019.116636

Hibender, S., Wanga, S., van der Made, I., Vos, M., Mulder, B. J. M., Balm, R., de Vries, C. J. M., & de Waard, V. (2019). Renal cystic disease in the Fbn1(C1039G/+) Marfan mouse is associated with enhanced aortic aneurysm formation. *Cardiovascular Pathology*, *38*, 1–6. https://doi.org/10.1016/j.carpath.2018.10.002

Hoshijima, K., Jurynec, M. J., Klatt Shaw, D., Jacobi, A. M., Behlke, M. A., & Grunwald, D. J. (2019). Highly efficient CRISPR-Cas9-based methods for generating deletion mutations and F0 embryos that lack gene function in zebrafish. *Developmental Cell*, *51*(5), 645–657.e644. https://doi.org/10.1016/j.devcel.2019.10.004

Howe, K., Clark, M. D., Torroja, C. F., Torrance, J., Berthelot, C., Muffato, M., Collins, J. E., Humphray, S., McLaren, K., Matthews, L., McLaren, S., Sealy, I., Caccamo, M., Churcher, C., Scott, C., Barrett, J. C., Koch, R., Rauch, G.-J., White, S., ... Stemple, D. L. (2013). The zebrafish reference genome sequence and its relationship to the human genome. *Nature*, *496*(7446), 498–503. https://doi.org/10.1038/nature12111

Jensen, S. A., & Handford, P. A. (2016). New insights into the structure, assembly and biological roles of 10–12 nm connective tissue microfibrils from fibrillin-1 studies. *The Biochemical Journal*, *473*(7), 827–838. https://doi.org/10.1042/bj20151108

Jondeau, G., Boileau, C., & Milleron, O. (2017). Marfan syndrome: Always evolving. *Circulation Cardiovascular Genetics*, *10*(3), https://doi.org/10.1161/circgenetics.117.001785

Jondeau, G., Michel, J. B., & Boileau, C. (2011). The translational science of Marfan syndrome. *Heart*, *97*(3), 1206–1214. https://doi.org/10.1136/hrt.2010.212100

Jones, J. A., & Ikonomidis, J. S. (2010). The pathogenesis of aortopathy in Marfan syndrome and related diseases. *Current Cardiology Reports*, *12*(2), 99–107. https://doi.org/10.1007/s11886-010-0083-z

Karoulias, S. Z., Beyens, A., Balic, Z., Symoens, S., Vandersteen, A., Rideout, A. L., Dickinson, J., Callewaert, B., & Hubmacher, D. (2020). A novel ADAMTS17 variant that causes Weill-Marchesani syndrome 4 alters fibrillin-1 and collagen type I deposition in the extracellular matrix. *Matrix Biology*, *88*, 1–18. https://doi.org/10.1016/j.matbio.2019.11.001

Kim, O. H., An, H. S., & Choi, T. Y. (2019). Generation of mmp15b zebrafish mutant to investigate liver diseases. *Development & Reproduction*, *23*(4), 385–390. https://doi.org/10.12717/dr.2019.23.4.385

Lamason, R. L., Mohideen, M. A., Mest, J. R., Wong, A. C., Norton, H. L., Aros, M. C., & Cheng, K. C. (2005). SLC24A5, a putative cation exchanger, affects pigmentation in zebrafish and humans. *Science*, *310*(5755), 1782–1786. https://doi.org/10.1126/science.1116238

Ledoux, M., Beauchet, A., Fermanian, C., Boileau, C., Jondeau, G., & Saiag, P. (2011). A case-control study of cutaneous signs in adult patients with Marfan disease: Diagnostic value of striae.

Journal of the American Academy of Dermatology, *64*(2), 290–295. https://doi.org/10.1016/j.jaad.2010.01.032

Li, J., Wu, W., Lu, C., Liu, Y., Wang, R., Si, N., Liu, F., Zhou, J., Zhang, S., & Zhang, X. (2017). Gross deletions in FBN1 results in variable phenotypes of Marfan syndrome. *Clinica Chimica Acta*, *474*, 54–59. https://doi.org/10.1016/j.cca.2017.08.023

Lin, M., Liu, Z., Liu, G., Zhao, S., Li, C., Chen, W., & Wu, N. (2020). Genetic and molecular mechanism for distinct clinical phenotypes conveyed by allelic truncating mutations implicated in FBN1. *Molecular Genetics & Genomic Medicine*, *8*(1), e1023. https://doi.org/10.1002/mgg3.1023

Lin, M., Zhao, S., Liu, G., Huang, Y., Yu, C., Zhao, Y., Wang, L., Zhang, Y., Yan, Z., Wang, S., Liu, S., Liu, J., Ye, Y., Chen, Y., Yang, X. U., Tong, B., Wang, Z., Yang, X., Niu, Y., ... Wu, N. (2020). Identification of novel FBN1 variations implicated in congenital scoliosis. *Journal of Human Genetics*, *65*(3), 221–230. https://doi.org/10.1038/s10038-019-0698-x

Liu, C.-X., Li, C.-Y., Hu, C.-C., Wang, Y. I., Lin, J., Jiang, Y.-H., Li, Q., & Xu, X. (2018). CRISPR/Cas9-induced shank3b mutant zebrafish display autism-like behaviors. *Molecular Autism*, *9*, 23. https://doi.org/10.1186/s13229-018-0204-x

Mastromoro, G., Guida, V., Cellitti, R., Cardilli, V., De Luca, A., Pizzuti, A., & Versacci, P. (2021). Neonatal Marfan syndrome by inherited mutation. *Indian Journal of Pediatrics*, *88*(2), 176–177. https://doi.org/10.1007/s12098-020-03411-y

Milleron, O., Arnoult, F., Delorme, G., Detaint, D., Pellenc, Q., Raffoul, R., Tchitchinadze, M., Langeois, M., Guien, C., Beroud, C., Ropers, J., Hanna, N., Arnaud, P., Gouya, L., Boileau, C., & Jondeau, G. (2020). Pathogenic FBN1 genetic variation and aortic dissection in patients with Marfan syndrome. *Journal of the American College of Cardiology*, *75*(8), 843–853. https://doi.org/10.1016/j.jacc.2019.12.043

Muthu, M. L., & Reinhardt, D. P. (2020). Fibrillin-1 and fibrillin-1-derived asprosin in adipose tissue function and metabolic disorders. *Journal of Cell Communication and Signaling*, *14*(2), 159–173. https://doi.org/10.1007/s12079-020-00566-3

Newell, K., Smith, W., Ghoshhajra, B., Isselbacher, E., Lin, A., & Lindsay, M. E. (2017). Cervical artery dissection expands the cardiovascular phenotype in FBN1-related Weill-Marchesani syndrome. *American Journal of Medical Genetics Part A*, *173*(9), 2551–2556. https://doi.org/10.1002/ajmg.a.38353

Park, J. H., Kim, M. S., Ham, S., Park, E. S., Kim, K. L., & Suh, W. (2019). Transforming growth factor β receptor type i inhibitor, galunisertib, has no beneficial effects on aneurysmal pathological changes in Marfan mice. *Biomol Ther (Seoul)*, *28*(1), 98–103. https://doi.org/10.4062/biomolther.2019.042

Piqueras-Flores, J., Trujillo-Quintero, J. P., Frías-García, R., González-Marín, M. A., Monserrat, L., & Hernández-Herrera, G. (2019). Incomplete mass phenotype: Description of a new pathogenic variant of the fibrillin-1 gene. *Revista Española De Cardiología (English Edition)*, *72*(10), 868–870. https://doi.org/10.1016/j.rec.2019.01.014

Ramirez, F., & Pereira, L. (1999). The fibrillins. *International Journal of Biochemistry & Cell Biology*, *31*(2), 255–259. https://doi.org/10.1016/S1357-2725(98)00109-5

Rantamäki, T., Karttunen, L., & Peltonen, L. (1997). Badly engineered fibrillin lessons from molecular studies of Marfan syndrome. *Trends in Cardiovascular Medicine*, *7*(8), 282–288. https://doi.org/10.1016/S1050-1738(97)00087-X

Richards, S., Aziz, N., Bale, S., Bick, D., Das, S., Gastier-Foster, J., Grody, W. W., Hegde, M., Lyon, E., Spector, E., Voelkerding, K., & Rehm, H. L. (2015). **S**tandards and guidelines for the interpretation of sequence variants: A joint consensus recommendation of the American College of Medical Genetics and Genomics and the Association for Molecular Pathology. *Genetics in Medicine*, *17*(5), 405–424. https://doi.org/10.1038/gim.2015.30

Robinson, P. N., Arteaga-Solis, E., Baldock, C., Collod-Beroud, G., Booms, P., De Paepe, A., Dietz, H. C., Guo, G., Handford, P. A., Judge, D. P., Kielty, C. M., Loeys, B., Milewicz, D. M., Ney, A., Ramirez, F., Reinhardt, D. P., Tiedemann, K., Whiteman, P., & Godfrey, M. (2006). The molecular genetics of Marfan syndrome and related disorders. *Journal of Medical Genetics*, *43*(10), 769–787. https://doi.org/10.1136/jmg.2005.039669

Sakai, L. Y., Keene, D. R., Renard, M., & De Backer, J. (2016). FBN1: The disease-causing gene for Marfan syndrome and other genetic disorders. *Gene*, *591*(1), 279–291. https://doi.org/10.1016/j.gene.2016.07.033

Sato, T., Arakawa, M., Tashima, Y., Tsuboi, E., Burdon, G., Trojan, J., Koyano, T., Youn, Y.-N., Penov, K., Pedroza, A. J., Shabazzi, M., Palmon, I., Nguyen, M. N., Connolly, A. J., Yamaguchi, A., & Fischbein, M. P. (2018). Statins reduce thoracic aortic aneurysm growth in marfan syndrome mice via inhibition of the ras-induced ERK (Extracellular Signal-Regulated Kinase) signaling pathway. *Journal of the American Heart Association*, *7*(21), e008543. https://doi.org/10.1161/jaha.118.008543

Schrenk, S., Cenzi, C., Bertalot, T., Conconi, M. T., & Di Liddo, R. (2018). Structural and functional failure of fibrillin-1 in human diseases (Review). *International Journal of Molecular Medicine*, *41*(3), 1213–1223. https://doi.org/10.3892/ijmm.2017.3343

Siegert, A. M., Serra-Peinado, C., Gutiérrez-Martínez, E., Rodríguez-Pascual, F., Fabregat, I., & Egea, G. (2018). Altered TGF-β endocytic trafficking contributes to the increased signaling in Marfan syndrome. *Biochimica Et Biophysica Acta (BBA) - Molecular Basis of Disease*, *1864*(2), 554–562. https://doi.org/10.1016/j.bbadis.2017.11.015

Sivasankari, T., Mathew, P., Austin, R. D., & Devi, S. (2017). Marfan syndrome. *Journal of Pharmacy and Bioallied Sciences*, *9*(1), 73–77. https://doi.org/10.4103/jpbs.JPBS_326_16

Smaldone, S., & Ramirez, F. (2016). Fibrillin microfibrils in bone physiology. *Matrix Biology*, *52–54*, 191–197. https://doi.org/10.1016/j.matbio.2015.09.004

Takeda, N., Hara, H., Fujiwara, T., Kanaya, T., Maemura, S., & Komuro, I. (2018). TGF-β signaling-related genes and thoracic aortic aneurysms and dissections. *International Journal of Molecular Sciences*, *19*(7), 2125. https://doi.org/10.3390/ijms19072125

Takeda, N., & Komuro, I. (2019). Genetic basis of hereditary thoracic aortic aneurysms and dissections. *Journal of Cardiology*, *74*(2), 136–143. https://doi.org/10.1016/j.jjcc.2019.03.014

Tan, L., Li, Z., Zhou, C., Cao, Y., Zhang, L., Li, X., Cianflone, K., Wang, Y., & Wang, D. W. (2017). FBN1 mutations largely contribute to sporadic non-syndromic aortic dissection. *Human Molecular Genetics*, *26*(24), 4814–4822. https://doi.org/10.1093/hmg/ddx360

Tessadori, F., Roessler, H. I., Savelberg, S. M. C., Chocron, S., Kamel, S. M., Duran, K. J., van Haelst, M. M., van Haaften, G., & Bakkers, J. (2018). Effective CRISPR/Cas9-based nucleotide editing in zebrafish to model human genetic cardiovascular

disorders. *Disease Models & Mechanisms*, *11*(10), dmm035469. https://doi.org/10.1242/dmm.035469

Tognato, E., Perona, A., Aronica, A., Bertola, A., Cimminelli, L., De Vecchi, S., Eshraghy, M. R., Loperfido, B., Vivenza, C., & Manzoni, P. (2019). Neonatal Marfan syndrome. *American Journal of Perinatology*, *36*(S 02), S74–S76. https://doi.org/10.1055/s-0039-1691770

Torraca, V., & Mostowy, S. (2018). Zebrafish infection: From pathogenesis to cell biology. *Trends in Cell Biology*, *28*(2), 143–156. https://doi.org/10.1016/j.tcb.2017.10.002

Tran, P. H. T., Skrba, T., Wondimu, E., Galatioto, G., Svensson, R. B., Olesen, A. T., Mackey, A. L., Magnusson, S. P., Ramirez, F., & Kjaer, M. (2019). The influence of fibrillin-1 and physical activity upon tendon tissue morphology and mechanical properties in mice. *Physiological Reports*, *7*(21), e14267. https://doi.org/10.14814/phy2.14267

Umeyama, K., Watanabe, K., Watanabe, M., Horiuchi, K., Nakano, K., Kitashiro, M., Matsunari, H., Kimura, T., Arima, Y., Sampetrean, O., Nagaya, M., Saito, M., Saya, H., Kosaki, K., Nagashima, H., & Matsumoto, M. (2016). Generation of heterozygous fibrillin-1 mutant cloned pigs from genome-edited foetal fibroblasts. *Scientific Reports*, *6*, 24413. https://doi.org/10.1038/srep24413

Varshney, G. K., Pei, W., LaFave, M. C., Idol, J., Xu, L., Gallardo, V., Carrington, B., Bishop, K., Jones, M. P., Li, M., Harper, U., Huang, S. C., Prakash, A., Chen, W., Sood, R., Ledin, J., & Burgess, S. M. (2015). High-throughput gene targeting and phenotyping in zebrafish using CRISPR/Cas9. *Genome Research*, *25*(7), 1030–1042. https://doi.org/10.1101/gr.186379.114

Vasques, G. A., Andrade, N. L. M., & Jorge, A. A. L. (2019). Genetic causes of isolated short stature. *Archives of Endocrinology and Metabolism*, *63*(1), 70–78. https://doi.org/10.20945/2359-3997000000105

Wang, J., Yan, Y., Chen, J., Gong, L., Zhang, Y. U., Yuan, M., Cui, B., & Wang, Y. (2016). Novel FBN1 mutations are responsible for cardiovascular manifestations of Marfan syndrome. *Molecular Biology Reports*, *43*(11), 1227–1232. https://doi.org/10.1007/s11033-016-4067-y

Xu, F. R., Jiang, W. J., Zhang, T., Jiang, Q., Zhang, R. X., & Bi, H. S. (2019). Fibrillin-2 gene mutations associated with hereditary connective tissue diseases. *Yi Chuan*, *41*(10), 919–927. https://doi.org/10.16288/j.yczz.19-052

Xu, S., Li, L., Fu, Y., Wang, X., Sun, H., Wang, J., Han, L. U., Wu, Z., Liu, Y., Zhu, J., Sun, L., Lan, F., He, Y., & Zhang, H. (2020). Increased frequency of FBN1 frameshift and nonsense mutations in Marfan syndrome patients with aortic dissection. *Molecular Genetics & Genomic Medicine*, *8*(1), e1041. https://doi.org/10.1002/mgg3.1041

Yang, Y., Zhou, Y. L., Yao, T. T., Pan, H., Gu, P., & Wang, Z. Y. (2020). Novel p. G1344E mutation in FBN1 is associated with ectopia lentis. *British Journal of Ophthalmology*, https://doi.org/10.1136/bjophthalmol-2019-315265

Zhang, Y., Jin, G., Young, C. A., Cao, Q., Lin, J., Lin, J., Wang, Y., & Zheng, D. (2018). Analysis of corneal astigmatism before surgery in Chinese congenital ectopia lentis patients. *Current Eye Research*, *43*(8), 972–976. https://doi.org/10.1080/02713683.2018.1470248

Zigrino, P., & Sengle, G. (2019). Fibrillin microfibrils and proteases, key integrators of fibrotic pathways. *Advanced Drug Delivery Reviews*, *146*, 3–16. https://doi.org/10.1016/j.addr.2018.04.019

SUPPORTING INFORMATION

Additional supporting information may be found online in the Supporting Information section.

How to cite this article: Yin, X., Hao, J., & Yao, Y. (2021). CRISPR/Cas9 in zebrafish: An attractive model for FBN1 genetic defects in humans. *Molecular Genetics & Genomic Medicine*, 9, e1775. https://doi.org/10.1002/mgg3.1775